



## Impact of the COVID-19 outbreak on urban air, Land surface temperature and air pollution in cold climate zones

Sevgi Yilmaz <sup>a,\*</sup>, Yaşar Menteş <sup>b</sup>, Sena Nur Angin <sup>c</sup>, Adeb Qaid <sup>d</sup>

<sup>a</sup> Atatürk University, Faculty of Architecture and Design, Department of Landscape Architecture, 25240 Erzurum, Turkey

<sup>b</sup> Ministry of Agriculture and Forestry, Elazığ Provincial Directorate of Agriculture and Forestry, Elazığ - PhD Candidate, Atatürk University, Faculty of Architecture and Design Department of Landscape Architecture Affiliation, Erzurum, Turkey

<sup>c</sup>, Atatürk University, Faculty of Architecture and Design, Department of Landscape Architecture, 25240 Erzurum, Turkey

<sup>d</sup> Department of Architecture Engineering, Kingdom University, Riffa, Bahrain



### ARTICLE INFO

Handling Editor: Jose L Domingo

**Keywords:**

COVID-19

Air temperature

Land surface temperature (LST)

Air pollution

Cold region

### ABSTRACT

The objective of this study was to analyze air pollution and thermal environment in Turkey's cold region before, during, and after COVID-19 in 2019, 2020 and 2021. The CO, NO<sub>2</sub>, O<sub>3</sub>, PM<sub>10</sub> and SO<sub>2</sub> data from the state air quality stations, as well as ground air temperature data from six weather stations, and land satellite images from the USGS website using ArcGIS 10.4.1 software were collected in January, March, April and August of 2019, 2020 and 2021. In order to evaluate the impact of COVID-19 measures and restrictions on cold region cities, air pollution indicators, land surface temperature and air temperature as well as statistical data were analyzed. The results indicated that the CO, NO<sub>2</sub>, PM<sub>10</sub> and SO<sub>2</sub> emissions decreased by 14.9%, 14.3%, 47.1% and 28.5%, but O<sub>3</sub> increased by 16.9%, respectively, during the COVID-19 lockdown in 2020 as compared to these of the pre-COVID-19 levels in 2019. A positive correlation between air temperature and O<sub>3</sub> in 2019 ( $r^2 = 0.80$ ), and in 2020 and 2021 ( $r^2 = 0.64$ ) was obtained. Air temperature in 2020 and 2021 decreased due to lockdowns and quarantine measures that led to lower O<sub>3</sub> emissions as compared to 2019. Negative correlations were also found between air temperature and NO<sub>2</sub> ( $r^2 = 0.60$ ) and SO<sub>2</sub> ( $r^2 = 0.5$ ). There was no correlation between air temperature and PM<sub>10</sub>. During the COVID-19 lockdown and intense restrictions in April 2020, the average LST and air temperature values dropped by 14.7 °C and 1.6 °C respectively, compared to April 2019. These findings may be beneficial for future urban planning, particularly in cold regions.

### 1. Introduction

According to data from the United Nations, the rate of urbanization in the world is increasing rapidly. Globally, the urban population increased from 751 million in 1950 to 4.2 billion in 2018, representing an increase of 4.6 times. It is estimated that this number will increase further and reach 6.4 billion in 2050 (UN, 2019; Huang et al., 2021). It must accommodate more than half of the world's population in just 3% of Earth's land surface area (UN, 2019). In parallel with this population increase in urban areas, the need for housing is also increasing rapidly. Cities, as a comprehensive phenomenon, are increasing their hard and impervious surfaces by building more every day to meet this demand. This situation of cities affects thermal comfort (Nikolopoulou and Steemers, 2003; Nikolopoulou and Lykoudis, 2006; Chandan et al., 2019; Bharath et al., 2019). The increasing population in urban areas,

automobile exhaust, impervious surfaces and dense housing texture also affect the urban climate. In fact, it has been determined that urban areas are warmer than rural areas due to these problems (Chen et al., 2014a; Unger, 1999; Jongtanom et al., 2011; Irmak et al., 2020; Yilmaz et al., 2021a). Land surface temperature (LST) has been used to assess the Urban Heat Island (UHI) and is a key parameter in controlling the temperature and air pollution between the atmosphere and the land surface. The surface temperatures of these areas, which have different directions and features, also have different temperatures (Amanollahi et al., 2016; Okumus and Terzi, 2021; Reis et al., 2022). Li et al. (2009) showed that the UHI patterns indicated by LSTs implied the existence of spatial correlation on the small and meso-scales. According to Zhou et al. (2018), rapid urbanization and economic development cause serious air pollution. One of the biggest problems people face in the 21st century is air pollution, which has many direct or indirect effects on human health

\* Corresponding author.

E-mail addresses: [sevgiy@atauni.edu.tr](mailto:sevgiy@atauni.edu.tr), [syilmaz\\_68@hotmail.com](mailto:syilmaz_68@hotmail.com) (S. Yilmaz), [adeebqaid@gmail.com](mailto:adeebqaid@gmail.com) (A. Qaid).

(Shehzad et al., 2021). As one of these effects, the report by WHO (2016) that there are 7 million premature deaths due to air pollution globally can be given as an example (Ravindra et al., 2022). The urban thermal field distribution in the winter directly affects the spread of air pollutants, which has important implications for analyzing the contribution of the thermal field to particulate air pollution. As studies measuring the levels of pollutants that adversely affect human health show, it has been stated that fossil fuels used for heating in cold climates and pollutants in the air that cause harm to human health cause air pollution (Wang et al., 2017; Shi et al., 2018; Li et al. 2019, 2022; Yilmaz et al. 2021b, 2022). It was determined that the death rates of the SARS epidemic in China were lower in areas with high air pollution, and the death rates were even higher than in areas with air pollution (Cui et al., 2003; Bray et al., 2021; Ekanayake et al., 2023). It has been stated that air pollution, which affects people's ability to fight infection and weakens the immune system, also affects COVID-19 (The European Public Health Alliance, 2020). People have realized over time that polluted air significantly impacts health, the economy and climate. It has been determined that air pollution significantly affects the aggravation of respiratory tract diseases (Ilyas et al., 2010).

COVID-19, which caused the epidemic that affected the whole world, is identified as the seventh member of the coronaviruses that infect humans (Bandyopadhyay, 2020; Zhu et al., 2020; Qaid et al., 2022). The World Health Organization (WHO) gave information about a new infectious disease that emerged in Wuhan, China, on December 31, 2019. In addition, it was announced that the COVID-19 epidemic was a global epidemic and was declared a pandemic (Fofana et al., 2020; Arslan et al., 2021; Qaid et al., 2022; Beloconi and Vounatsou, 2023). This virus, which affected the whole world, was first seen in Turkey on March 11, 2020 (Turkiye Ministry of Health, 2020).

Numerous academic studies on evaluating the impact of COVID-19 on air pollution have been carried out with some indicating that restrictions imposed during the pandemic have led to improved air quality (Venter et al., 2020; Mor et al., 2021). It has also been suggested that the use of masks may have a positive impact on human health in areas with air pollution. Among the anthropogenic factors, reduced traffic and air transportation have been identified as significant contributors to reductions in air pollution during the pandemic (Ravindra et al., 2022; Bao and Zhang, 2020). Other studies have shown that the greatest impact on air pollution was attributed to anthropogenic factors, with micro meteorological parameters also playing a role (Wang et al., 2020; Yilmaz et al., 2022; Zoran et al., 2022). A study conducted in Indonesia by Rendana et al. (2021) found a significant relationship between meteorological factors and the spread of the COVID-19 epidemic. Table 1 provides a summary of studies conducted worldwide on the effects of COVID-19 on air pollution. However, there are limited studies on the impact of COVID-19 on air pollution and the thermal environment in cold climates, with restricted methods, variables, and time periods to evaluate their effects. This study analyzed the major air pollution factors ( $\text{CO}$ ,  $\text{NO}_2$ ,  $\text{O}_3$ ,  $\text{PM}_{10}$ , and  $\text{SO}_2$ ) in a cold climate during COVID-19 in 2020, compared with data from 2019 to 2021, and their impact on air temperature and surface temperature LST was investigated. A combination of satellite data from Landsat 8, field measurements, climate data, and air pollution data were utilized along with statistical analysis for evaluating the data.

Several studies have explored the link between air pollution, climate change and meteorological parameters, including temperature, relative humidity and solar radiation, in the context of COVID-19 (Sicard et al., 2020; Allu et al., 2021; Ekanayake et al., 2023). Additionally, in a study carried in nine European cities, including Rome and Valencia, it was reported that the percentage increase in all-natural cause deaths per  $^{\circ}\text{C}$  rise in air temperature tended to be higher on days with high  $\text{O}_3$  levels (Analitis et al., 2018), indicating potential interactions with climate change.

In Erzurum City, the first case was recorded at the end of March (Erzurum Health Directorate, 2020). As of March 2020, some measures

have been taken across the country. Among these measures are the closure of schools, the prohibition of going out, the complete cancellation of intercity transportation, and the prohibition of going abroad. After a three-week break, schools switched to online education. However, other restrictions remained (Ministry of Education, 2020). In the following period, previously limited national and international flights were stopped entirely. In addition, a curfew was imposed between 19.00 and 05.00 on weekdays and throughout the weekend. Full closure was declared until 05:00 on 17 May 2021 and was implemented from 19:00 on 29 April 2021 (Ministry of Education, 2021).

This study aims to reveal the effects of the measures and restrictions taken within the scope of the epidemic that emerged at the end of 2019 on the air pollution, surface temperature, and air temperature of the city. Land surface temperature (LST) and air temperature are vital aspects of urban environmental quality and indicators of urban climate. Therefore, we propose to answer the question: How did COVID-19 pandemic measures and restrictions affect air pollution, land surface temperatures, and air temperatures in cold cities? This question formed the basis of this research. Air temperature, land surface temperature, and air pollution analyses should be performed to reduce air pollution and improve thermal comfort conditions for both summer and winter, especially in cities with these conditions in winter. These results may be useful for future urban planning, especially in cold regions.

## 2. Materials and methods

### 2.1. Location of the case study

This research was carried out in Erzurum, a city in the eastern Anatolian region of Turkey, which hosted the 2011 Winter Olympics and has important facilities in terms of winter tourism. The study area location map is given in Fig. 1.

The period with the lowest wind speed is January, with an average value of 1.9 m/s, and the highest period is August, with an average value of 4.2 m/s. When the region's wind regime is examined in terms of the fastest-blown winds and their arrival directions, it is seen that the annual average speed of high-speed winds reaches 2.7 m/s. The dominant wind direction in Erzurum and its surroundings is the southwest (SW) direction. Wind speed measurement data were recorded with the Trotec Ba16 anemometer device and kept at 1.1 m from the street floor. The wind characteristics of the study area are given in Fig. 2 (MGM, 2019; 2021; Sari and Yilmaz, 2021).

The city of Erzurum is located in the cold climate zone according to the Köppen criteria. The city, which has a continental climate, has an annual average temperature of  $6.0\ ^{\circ}\text{C}$ . The average of the coldest month is  $-8.3\ ^{\circ}\text{C}$ , and the average of the warmest month is  $20.2\ ^{\circ}\text{C}$ . Its precipitation is irregular, and the average annual precipitation is 460.5 mm (MGM, 2019). In this city surrounded by mountains, there is intense air pollution, especially in winter. Slump inversion frequently occurs in foothills and valleys. In clear weather and calm windy conditions and under high-pressure conditions, the cold air layer coming onto mountain skirts or valleys from a high region, such as a hill, mountainous region, or an obstacle is compressed as it descends from the high region and causes the compressed air mass to warm up. Thus, the ground's warm air layer at a certain height creates an inversion layer. This layer prevents the air mass and pollutants from rising and dispersing further (MoEU, 2017, 2022). In Erzurum, such inversions generally occur more frequently in winter and autumn. The use of poor-quality fuel for heating, faulty combustion systems, and vehicles consuming excessive fuel in transportation increase air pollution.

### 2.2. Methods

Three different methods were used in data collection for identifying effects of COVID-19 on the air and land surface temperatures and air pollution. Landsat 8 satellite-derived measurements of LST and ground-

**Table 1**

Some studies on the impact of the COVID-19 outbreak on air pollution.

Authors	City, Country	Climate of the city	Variables of the study	Climate and thermal variables	Methodology	Years of the study	Period of the study	Results of the study
Dutheil et al. (2020)	Central, China	Cold	Air pollution variables	–	Remote sensing and Sentinel-5 data	2020	2 months	NO <sub>2</sub> emissions were reduced by up to 30% and CO <sub>2</sub> emissions by 25%.
Liu et al. (2021)	597 major cities worldwide	Worldwide	Air pollution variables	–	Air pollution data and weather data	2020	1 January – 5 May	Compared to the pre-quarantine period, NO <sub>2</sub> decreased 23–37%, PM <sub>10</sub> 14–20%, SO <sub>2</sub> 2–20%, PM <sub>2.5</sub> 7–16% and CO 7–11%. However, O <sub>3</sub> increased by 10–27%.
Mete et al. (2022)	Adana, Turkey	Hot climate	Air pollution variables	–	Air pollution data from the National Air Quality Monitoring Network	2019–2020	1 March – 1 May	Compared to 2019, PM <sub>10</sub> decreased 0.35%, SO <sub>2</sub> 23.6%, CO 84%, NO <sub>x</sub> 46.5%, NO 34.5%, NO <sub>2</sub> 63.1% and O <sub>3</sub> 68.4% in 2020
Garcia et al. (2022)	Eight cities in Andalusia, Spain	Mediterranean Oceanic climate (Csb), Mediterranean climate (Cs), cold semi-arid climate	Air pollution variables	LST, air temperature	Sentinel 3 satellite thermal images and weather data	2019–2020	08 March 2019–20 June 2020	During the confinement period, average reductions of some environmental pollutants were achieved: SO <sub>2</sub> (~33.5%), PM <sub>10</sub> (~38.3%), NO <sub>2</sub> (~44.0%) and CO (~26.5%). However, the environmental variable O <sub>3</sub> underwent an average growth of 5.9%. The LST showed an average reduction of -4.6 °C (~19.3%)
Nakada and Urban (2020)	Sao Paulo, Brazil	Hot climate	Air pollution variables	–	Data from three air quality stations, remote sensing and S5p/TROPOMI	2019–2020	25 February 2019–24 March 2020	Drastic reductions on NO (up to ~77.3%), NO <sub>2</sub> (up to ~54.3%), and CO (up to ~64.8%) concentrations were observed in the urban area during partial lockdown compared to the five-year monthly mean. By contrast, an increase of approximately 30% in ozone concentrations was observed in urban areas
Bray et al. (2021)	Europe, USA, China, and India	Worldwide	Air pollution variables	–	Satellite observations and ground-based measurements	2020	March–April 2020	Global NO <sub>2</sub> column observations were reduced by approximately 9.19% (March) and 9.57% (April). Most monitoring sites in Europe, USA, China, and India showed declines in pollutant concentrations. Four major cities case studies also show a similar reduction trends and an increase in ozone concentration.
Sicard et al. (2020)	Rome and Turin in Italy, Nice in France, Valencia in Spain, Wuhan in China	Worldwide	Air pollution variables	–	Data from air monitoring stations	2020	1 January – 18 April	The lockdown caused a substantial reduction in NO <sub>x</sub> in all cities (~56%). Reductions in PM were much higher in Wuhan (~42%) than in Europe (~8%). The lockdown caused an ozone increase in all cities (17% in Europe, 36% in Wuhan)
Allu et al. (2021)	Hyderabad City, India	tropical wet and dry climate	Air pollution variables	Relative humidity and solar radiation	The software Envitas given by Thermo Fisher	2018–2019–2020	1 February–30 April	O <sub>3</sub> concentration increased from 26 ppb (by volume) to 56.4 ppb during pre-lockdown and lockdown period, respectively, due to the decrease in CO and NO <sub>x</sub> concentration. The concentration of NO <sub>2</sub> , NO and CO were also reduced during the lockdown period by 33.7%, 53.8% and 27.25%, respectively.

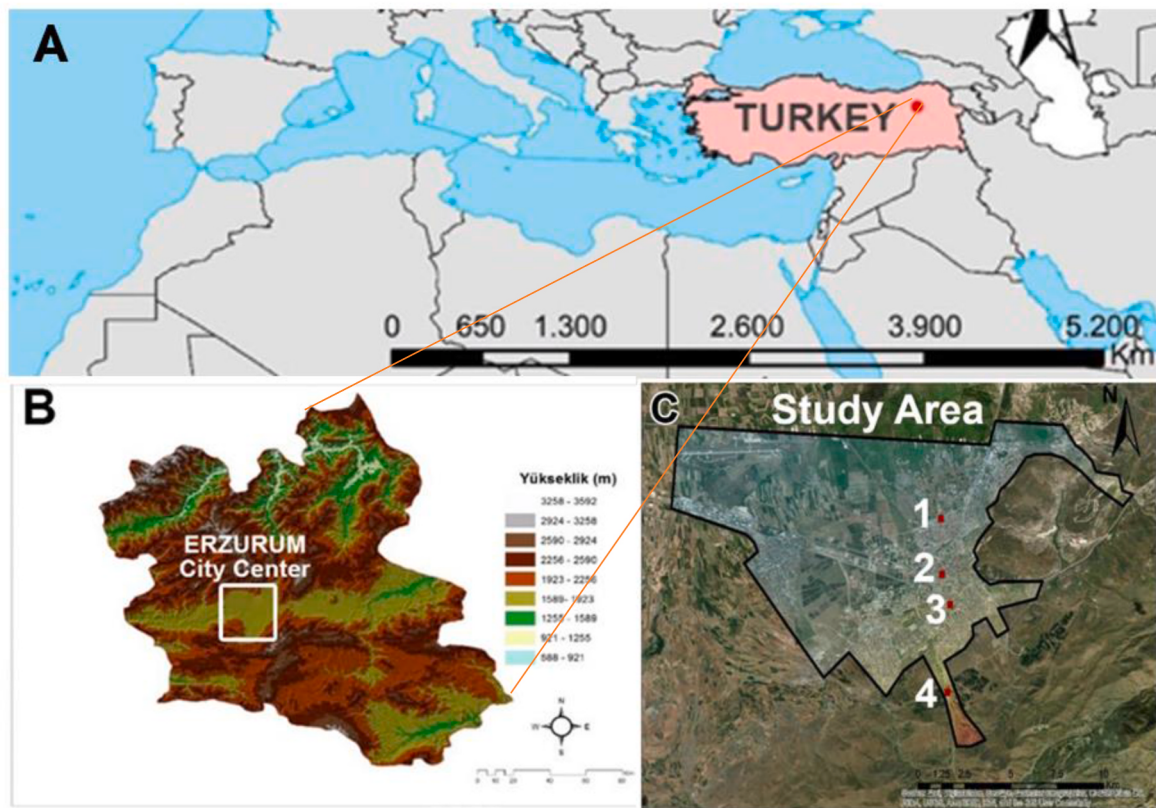


**Fig. 1.** A) Location of the country, B) Erzurum city environment topography, C) City center study area and red dots pollution measurement stations location map, (1) Aziziye Station, (2) Taşhan Station, (3) Central Station, (4) Palandöken Station.

based data of air pollution are used to provide a comprehensive estimate of the impact of the lockdown on air temperature in Erzurum. According to the station data, the hottest and coldest months were preferred for many years (MGM, 2019). The study period spanned from 1 January 2019 to 31 August 2021. In particular, the pre-and post-COVID-19 effects were analyzed. To determine the effect of the city with high air pollution in line with the measures and restrictions taken during the pandemic process, the years 2019–2020 and 2021 were selected to analyze air pollution. Intense restrictions and measures began in March 2020. Therefore, the restriction was also analyzed one year before and one year after. The effects of these measures on air pollution and surface temperature were examined within the scope of COVID-19 measures, curfews, travel bans, closure of restaurants, etc. Field measurement data were used to determine air pollution. Before and after restriction, five parameters, namely, CO, NO<sub>2</sub>, O<sub>3</sub>, PM<sub>10</sub>, and SO<sub>2</sub> values, were examined. The field measurement data were obtained from the Central, Aziziye, Taşhan, and Palandöken stations of Erzurum Province. The meteorological data analyzed temperature before and after the pandemic from 2019 to 2021. Thirteen stations and 3 government-owned meteorology stations were located in the city center for this research. These are described below. The workflow of the methodology is shown in Fig. 3.

#### 2.2.1. Air pollution parameters from the ground station

The primary source of air pollution in the cold climate zone study area is the use of heating fuel during winter months. The Ministry of Environment and Urbanization monitors four air pollution stations in the city center, namely, Aziziye Station, Taşhan Station, Central Station, and Palandöken Station, which take hourly measurements. Further details about these stations are provided in Table 2 (Sari and Yilmaz, 2021). The study uses GIS to map the pollution data obtained, which were taken from the open-access website of the ministry (link: sim. csb.gov.tr). The air pollutants measured from space include Carbon (CO),

Nitrogen Dioxide (NO<sub>2</sub>), Ozone (O<sub>3</sub>), Particulate matter (PM<sub>10</sub>), and Sulfur dioxide (SO<sub>2</sub>).

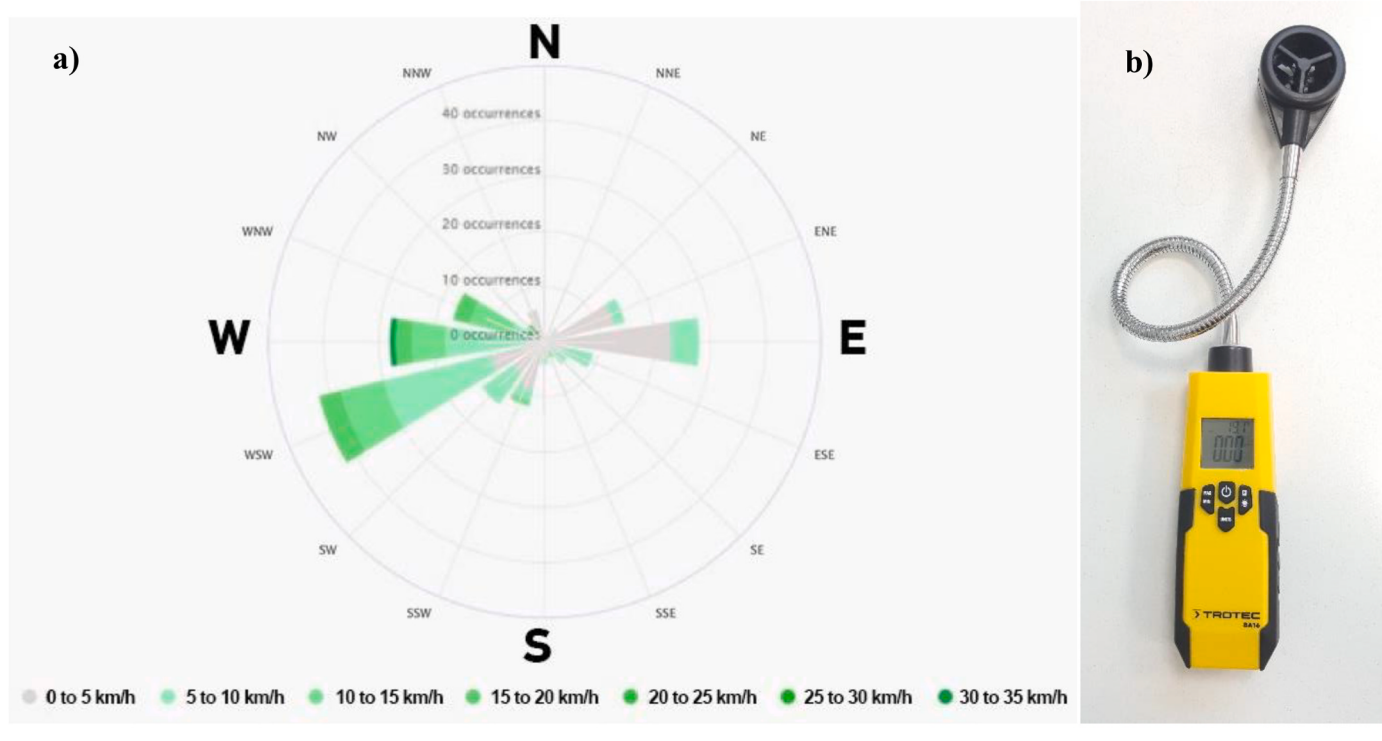
#### 2.2.2. Land surface temperature with thermal band

Remote sensing techniques are widely used in the analysis of land surface temperature (LST). These studies, which can cover the entire city or its immediate surroundings, are high-scale studies. Within the scope of the study, Landsat 8 satellite images downloaded from the USGS website (<https://earthexplorer.usgs.gov>) were used to calculate the Erzurum Province (LST) values.

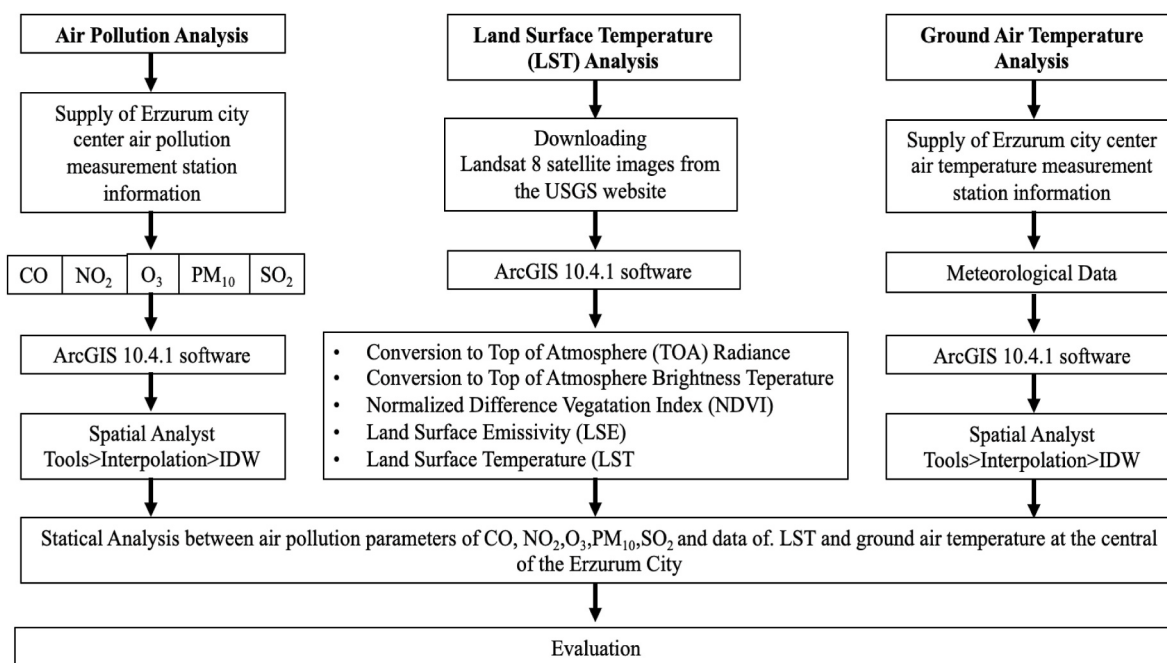
The collaboration between the National Aeronautics and Space Administration (NASA) and the United States Geological Survey (USGS) gave birth to Landsat 8, the eighth satellite under NASA's umbrella. Landsat 8 plays a crucial role in the management, monitoring, and comprehension of resources that are vital to human life, such as forests, water, and food. The Landsat program's significance is maintained through Landsat 8's capability to capture images within the visible, near-infrared, shortwave infrared, and thermal infrared ranges, with a medium spatial resolution varying from 15 to 100 m, depending on the spectral range. Hence, Landsat 8 offers medium-resolution data ranging from 15 to 100 m.

The Landsat 8 satellite has varying pixel resolutions of 15 m, 30 m, and 100 m for panchromatic, multispectral, and thermal ranges, respectively. Its image capture capability has significantly increased to 400 images per day, compared to Landsat 7's 250 daily captures. Furthermore, the TIRS sensors of Landsat 8 produce 12-bit images with superior signal-to-noise radiometric performance (Anonymous, 2023).

The Landsat 8 satellite is equipped with two sensors, namely, the Operational Land Imager (OLI) and the Thermal Infrared Sensor (TIRS). The OLI sensor is an upgraded version of the Advanced Land Imager (ALI) sensor found on NASA's EO-1 satellite, which was developed from previous Landsat sensors. It uses pushbroom technology instead of the



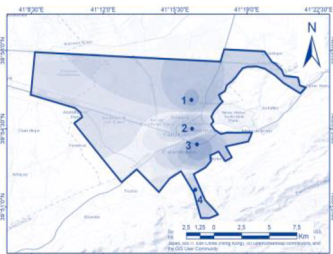
**Fig. 2.** a) Long-term data average wind rose; b) Wind anemometer device; c) Average wind speed and directions based on long-term data (MGM, 2019; Sari and Yilmaz, 2021).



**Fig. 3.** Workflow of the methodology.

**Table 2**

Erzurum city center air pollution measurement station information (Central Directorate of Clean Air for Eastern Anatolia- Sari and Yilmaz, 2021).

Air Quality Measurement Stations	Features
<b>Area Of The Study</b> 	<b>1 Aziziye Station</b> 2 Taşhan Station 3 Central Station 4 Palandöken Station
<b>(1) Aziziye Station</b> 	<b>Station Location Information</b> It was established on the State Railways in the south of the Mahrükatçilar site of the Yakutiye District of Erzurum Province in 2016. <b>Setup Date</b> Location of the station Coordinates; Latitude: 39°55'47.16" Longitude: 41°16'17.91" Altitude: 1823 <a href="https://www.havaizleme.gov.tr">https://www.havaizleme.gov.tr</a> is 225 m north-west of the indicated location <b>Weld Type And Measured Parameters</b> Warming-Field Welding From January – 2016 p.m.10, SO <sub>2</sub> , NO, NO <sub>2</sub> , NOx, and CO parameters Since the location of the station is located in the city center where the population and housing is dense, it exemplifies the air pollution caused by heating in the urban area.
<b>(2) Taşhan Station</b> 	<b>In 2016, Erzurum Province, Yakutiye District, Menderes Cad. It was established in front of Taşhan.</b> <b>Location of the station</b> Coordinates; Latitude: 39°54'29.60" Longitude: 41°16'19.86" Altitude: 1899 <a href="http://www.havaizleme.gov.tr">www.havaizleme.gov.tr</a> 55 m north-west of the indicated location <b>Traffic – Moving Source</b> As of January 2016, PM <sub>10</sub> , PM <sub>2.5</sub> , NO, NO <sub>2</sub> , NOx, and CO parameters are measured. Station; It exemplifies the air pollution caused by both traffic, population density, and heating in the urban area density in the city center.
<b>(3) Central Station</b> 	<b>In 2006, Erzurum Province, Yakutiye District Public Health (Hifzissihha) Lab. was established in its garden.</b> <b>Location of the station</b> Coordinates; Latitude: 39°53'47.62" Longitude: 41°16'34.02" Altitude: 1956 The location of the station is in the specified place at <a href="https://www.havaizleme.gov.tr">www.havaizleme.gov.tr</a> <b>Warming-Field Welding</b> PM <sub>10</sub> and SO <sub>2</sub> were added in April 2006, and NO, NO <sub>2</sub> , NOx, and O <sub>3</sub> parameters were added in Feb. 2016. Since the station has the highest traffic, workplace, residence, and population density in the city center, it exemplifies the air pollution caused by traffic and heating in the urban area.
<b>Palandöken Station</b> 	<b>It was established in 2016 near the Ski Center in Erzurum Province, Palandöken District.</b> <b>Location of station</b> Coordinates; Latitude: 39°51'45.64" Longitude: 41°16'29.38" Altitude: 2201 <a href="https://www.havaizleme.gov.tr">www.havaizleme.gov.tr</a> is 155 m South of the indicated location <b>Background-Out of Urban Area</b> As of January-2016, in addition to the air quality parameters PM <sub>10</sub> , SO <sub>2</sub> , NO, NO <sub>2</sub> , NOx, CO and O <sub>3</sub> , Temperature, Wind Direction, Wind Speed, Relative Humidity and Air Pressure are measured.

older whiskbroom sensor design, resulting in higher sensitivity, access to more detailed surface information, and fewer moving parts. (Anonymous, 2023).

According to the average temperature in years, the hottest and coldest months were chosen. Additionally, the month the pandemic and restrictions started and afterwards were chosen. Landsat satellite images of the province of Erzurum for January, March, April and Ağustos 2019, 2020 and 2021 were downloaded (Table 3). Arc GIS 10.4.1 software was used to prepare and evaluate LST maps. Cloudless and clear days were

selected to determine the day to be analyzed. It is a reliable analysis method widely used to determine surface temperature (Chen et al., 2014; Du et al., 2017; Shanshan et al., 2022).

**Performing LST analysis,** Band 10 (Thermal-1), Band 4 (red) and Band 5 (near infrared) are used to calculate the LST for Landsat 8 satellite images. LST values were calculated using the method developed by Chen et al. (2014b), Avdan and Jovanovska (2016) and Du et al. (2017) to determine the effect of LST in Erzurum.

The steps of this method are given below:

**Table 3**

Information on the Landsat 8 images used in the research.

Acquisition Date	Path	Row	Day/Night Indicator	Data Type Level-1	Land Cloud Cover (%)	Grid Cell Size Reflective	Grid Cell Size Thermal
28.01.2019	172	32	Day	OLI_TIRS_L1TP	18.62	30.00	30.00
01.03.2019	172	32	Day	OLI_TIRS_L1TP	41.76	30.00	30.00
11.04.2019	172	32	Day	OLI_TIRS_L1TP	28.32	30.00	30.00
08.08.2019	172	32	Day	OLI_TIRS_L1TP	15.63	30.00	30.00
15.01.2020	172	32	Day	OLI_TIRS_L1TP	0.14	30.00	30.00
03.03.2020	172	32	Day	OLI_TIRS_L1TP	1.55	30.00	30.00
04.04.2020	172	32	Day	OLI_TIRS_L1TP	43.68	30.00	30.00
26.08.2020	172	32	Day	OLI_TIRS_L1TP	0.13	30.00	30.00
01.01.2021	172	32	Day	OLI_TIRS_L1TP	4.74	30.00	30.00
06.03.2021	172	32	Day	OLI_TIRS_L1TP	4.20	30.00	30.00
23.04.2021	172	32	Day	OLI_TIRS_L1TP	3.15	30.00	30.00
29.08.2021	172	32	Day	OLI_TIRS_L1TP	0.01	30.00	30.00

**a Conversion to Top of Atmosphere (TOA) Radiance**

$$L\lambda = ML * Q_{cal} + AL - Oi \quad (1)$$

 $L\lambda$  = TOA spectral radiance (Watts/(m<sup>2</sup> \* srad \* μm))

ML = Band-specific multiplicative rescaling factor from the metadata (RADIANC\_MULT\_BAND\_x, where x is the band number).

AL = Band-specific additive rescaling factor from the metadata (RADIANC\_ADD\_BAND\_x, where x is the band number).

Qcal = Quantized and calibrated standard product pixel values (DN).

Oi: Correction value for band 10.

**b Conversion to Top of Atmosphere (TOA) Brightness Temperature (BT)**

$$BT = \left( \frac{K2}{\ln\left(\frac{K1}{L\lambda}\right)} + 1 \right) - 273,15 \quad (2)$$

BT = Top of atmosphere brightness temperature (°C).

 $L\lambda$  = TOA spectral radiance (Watts/(m<sup>2</sup> \* srad \* μm))

K1=K1 Constant Band (No.)

K2=K2 Constant Band (No.)

**c Normalized Difference Vegetation Index (NDVI)**

$$NDVI = \frac{NIR(Band5) - R(Band4)}{NIR(Band5) + R(Band4)} \quad (3)$$

NIR = DN values from Near-Infrared band.

R = DN values from the RED band.

**d Land surface emissivity (LSE)**

$$Pv = \left( \frac{NDVI - NDVImin}{NDVImax - NDVImin} \right)^2 \quad (4)$$

Pv = Proportion of Vegetation.

NDVI = Dn values from NDVI Image.

NDVImin: Minimum Dn values from NDVI Image.

NDVImax: Maximum Dn values from NDVI Image

$$\epsilon = 0.004 * Pv + 0.976 \quad (5)$$

 $\epsilon$  = Land surface emissivity.

Pv = Proportion of Vegetation.

0.976 corresponds to a correction value of the equation.

**e Land Surface Temperature (LST)**

Land Surface Temperature (LST) is the radiative temperature Which calculated using Top of atmosphere brightness temperature, Wavelength of emitted radiance, Land Surface Emissivity.

$$LST = \frac{BT}{1 + \left( \frac{\lambda \cdot BT}{c^2} \right) \cdot \ln(\epsilon)} \quad (6)$$

BT = Top of atmosphere brightness temperature (°C).

 $\lambda$  = Wavelength of emitted radiance $\epsilon$  = Land surface emissivity $\epsilon = 0.004 * Pv + 0.976$ .

Pv = Proportion of Vegetation

 $c^2 = h^*c/s = 1.4388 * 10^{-2}$  mK $h$  = Planck's constant =  $6.626 * 10^{-34}$  Js $s$  = Boltzmann constant =  $1.38 * 10^{-23}$  J/K $c$  = Velocity of light =  $2.998 * 10^8$  m/s.**2.2.3. Ground air temperature stations**

The weather data of the 16 meteorological stations in Erzurum for the months of 2019, 2020, and 2021 January, March, April, and August were used. For comparison in this study, the same months were chosen. Temperature data (air temperature °C-Ta) Using the Vantage Pro2 Meteorology station EU version instrument. Each station was enclosed in wire cages to avoid damage. The stations are installed in a shielded wire cage at a height of 1.5 m from the ground. Hourly data are mapped in the GIS environment. Arc-GIS 10.2 package program (Koç and Yilmaz, 2020). It has been determined that there is a significant relationship between temperature and urban texture (De and Mukherjee, 2018; Javanroodi and Nik, 2020). The locations of the 16 stations used in this study are shown in Fig. 4. Maximum, minimum, and average air temperature maps of these months were obtained with the ArcGIS 10.4.1 program. IDW was used to create air temperature maps (Weng et al., 2007).

**3. Results and discussion**

Land surface temperature with thermal band analysis, ground air pollution, and ground air temperature analysis was performed to determine the surface temperature for the distribution of air pollution parameters for Erzurum.

**3.1. Land surface temperature with thermal band analysis**

The thermal band analysis mapping used the data for 2019, 2020 and 2021, January, March, April, and August (Fig. 5). Since each object has different temperatures using the thermal infrared bands of Landsat TM 8 data, the urban objects are classified using the land surface temperature map. For local studies of UHIs, the TIR data of Landsat Thematic Mapper (TM) and Enhanced Thematic Mapper Plus (ETM+) with 120 m and 60 m spatial resolutions, respectively, were also utilized. LST changes over a specific area are highly variable and sensitive to many parameters, such as topography, altitude, slope, vegetation cover, type of vegetation, soil moisture, roughness, surface albedo, and absorptivity, which are closely related to land use type (Harmay et al., 2021). Therefore, LST

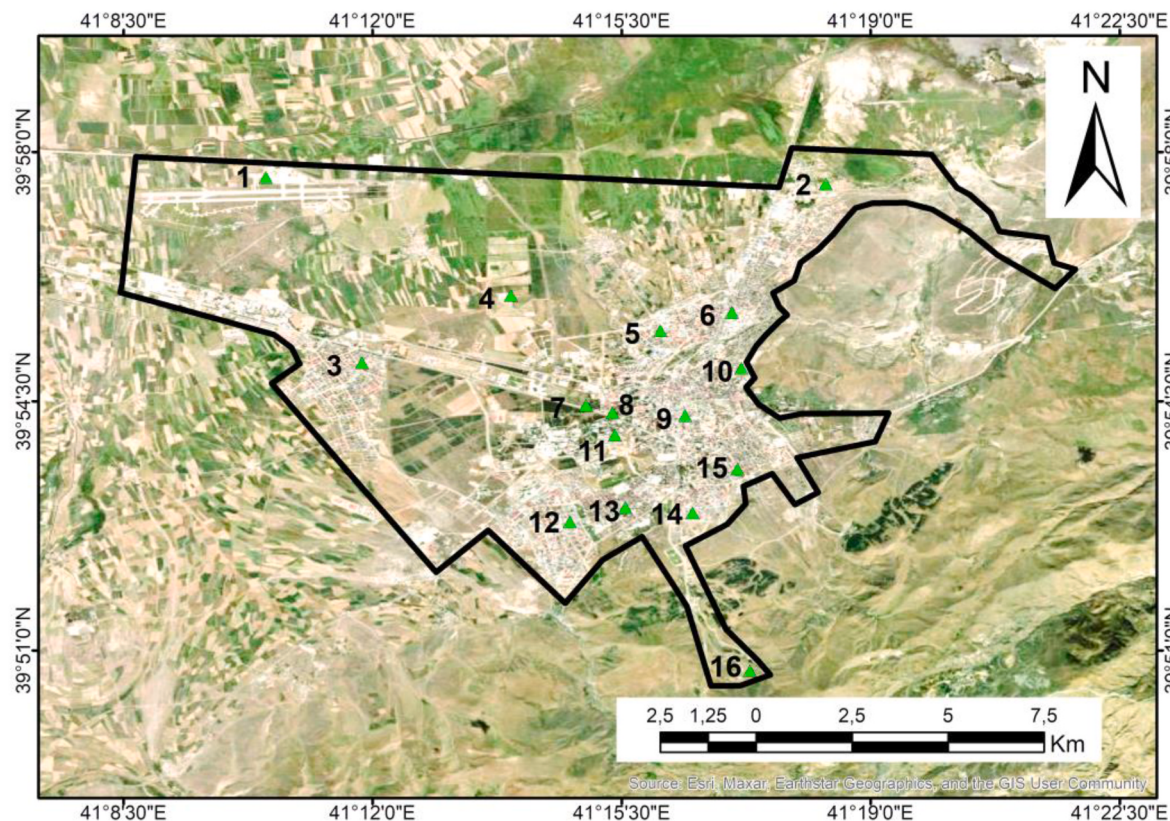


**Fig. 4.** Erzurum city center air temperature measurement station location map: (1) State Airports Authority Station, (2) Seasonal Wetland Station, (3) Dadaşkent Station, (4) Çiftlik Neighborhood Station, (5) Şükrüpaşa Station, (6) Sanayi Station, (7) ATA Botanical Garden Station, (8) Meteorology General Directorate, (9) Yakutiye Station, (10) Dağ Neighborhood Station, (11) Atatürk University Station, (12) Yıldız Station, (13) Yenişehir Station, (14) Kayakyolu Station, (15) Yunus Emre Neighborhood Station, (16) Palandöken Station.

anomalies during the lockdown period may be sensitive to factors beyond the effect of fewer anthropogenic aerosols and pollutants in urban areas (Parida et al., 2021). In Montreal, Canada, a decrease in the near-surface temperature was found to be approximately  $-1.0^{\circ}\text{C}$ , associated with an approximately 80% reduction in traffic (Teufel et al., 2021). Local weather conditions are one of the fundamental drivers of LST development (Yang et al., 2020). The surface temperature values and meteorological data obtained from ground measurements do not overlap. Surface temperature analysis gives instantaneous values that vary according to the time the satellite passes. Ground measurement values from meteorology express the values obtained with a vehicle target. Satellite images pass the same spot at different times every sixteen days (Guha et al., 2020; Shanshan et al., 2022). For this reason, it is considered normal that the data do not overlap with each other.

The COVID-19 pandemic provided a unique opportunity to investigate the impact of human activities on environmental pollution and their potential effects on the urban climate, particularly with respect to Land Surface Temperature (LST) (García and Díaz, 2022).

Table 4 data reveals differences in surface temperature across years and months. The surface temperature analysis showed that the lowest average temperature in winter was  $-11.1^{\circ}\text{C}$  in January 2020. The warmest year in January was of 2019, with an average temperature of  $-5.8^{\circ}\text{C}$ .

In March, the highest surface temperature was recorded in 2020 with an average of  $1.0^{\circ}\text{C}$ , while 2019 had the coldest year with an average of  $-11.0^{\circ}\text{C}$ . In April, the highest surface temperature was recorded in 2021, with an average of  $26.3^{\circ}\text{C}$ , while the coldest year was 2020, with an average of  $-2.4^{\circ}\text{C}$ .

In August, the highest surface temperature was recorded in 2021, with an average of  $33.3^{\circ}\text{C}$ . During this period, the pandemic restrictions

were most intense after March 2020, and the surface temperature increased from  $31.8$  to  $33.3^{\circ}\text{C}$ , which corresponds to a  $1.5^{\circ}\text{C}$  increase. In this year, the maximum surface temperature of  $43.1^{\circ}\text{C}$  was observed, indicating heat stress (Table 4).

The average surface temperatures for March, April, and August in 2021 were higher than the average surface temperatures for the same months in 2019. However, for January, the average surface temperatures in 2019 were higher than those in 2021.

### 3.2. Ground air pollution data analysis

Pollution parameters and distribution maps for 2019, 2020, and 2021 obtained from four fixed air pollution measurement stations in Erzurum city center were prepared 1- Aziziye Station, 2- Taşhan Station, 3- Central Station, 4- Palandöken Station. While obtaining the maps, CO, NO<sub>2</sub>, O<sub>3</sub>, PM<sub>10</sub>, and SO<sub>2</sub> from air pollution parameters were analyzed. Images of these are given in Fig. 6.

Fig. 6 and Table 5 display the distribution and concentration of air pollutants (CO, NO<sub>2</sub>, O<sub>3</sub>, PM<sub>10</sub>, and SO<sub>2</sub>) for January, March, April, and August before (2019), during (2020), and after (2021) the COVID-19 pandemic. The data indicates a significant reduction in air pollution levels during the COVID-19 period in 2020, with lower minimum, maximum, and average rates compared to 2019 and 2021. However, the average data was analyzed, which represents the actual emission over the months. The average distribution of CO for the years 2019, 2020, and 2021 was  $647.16$ ,  $550.68$ , and  $552.7 \mu\text{g}/\text{m}^3$ , respectively. The highest average CO distribution was observed in 2019, which decreased during the COVID-19 period in 2020 but began to increase again after 2021.

The average distribution of NO<sub>2</sub> for the years 2019, 2020, and 2021

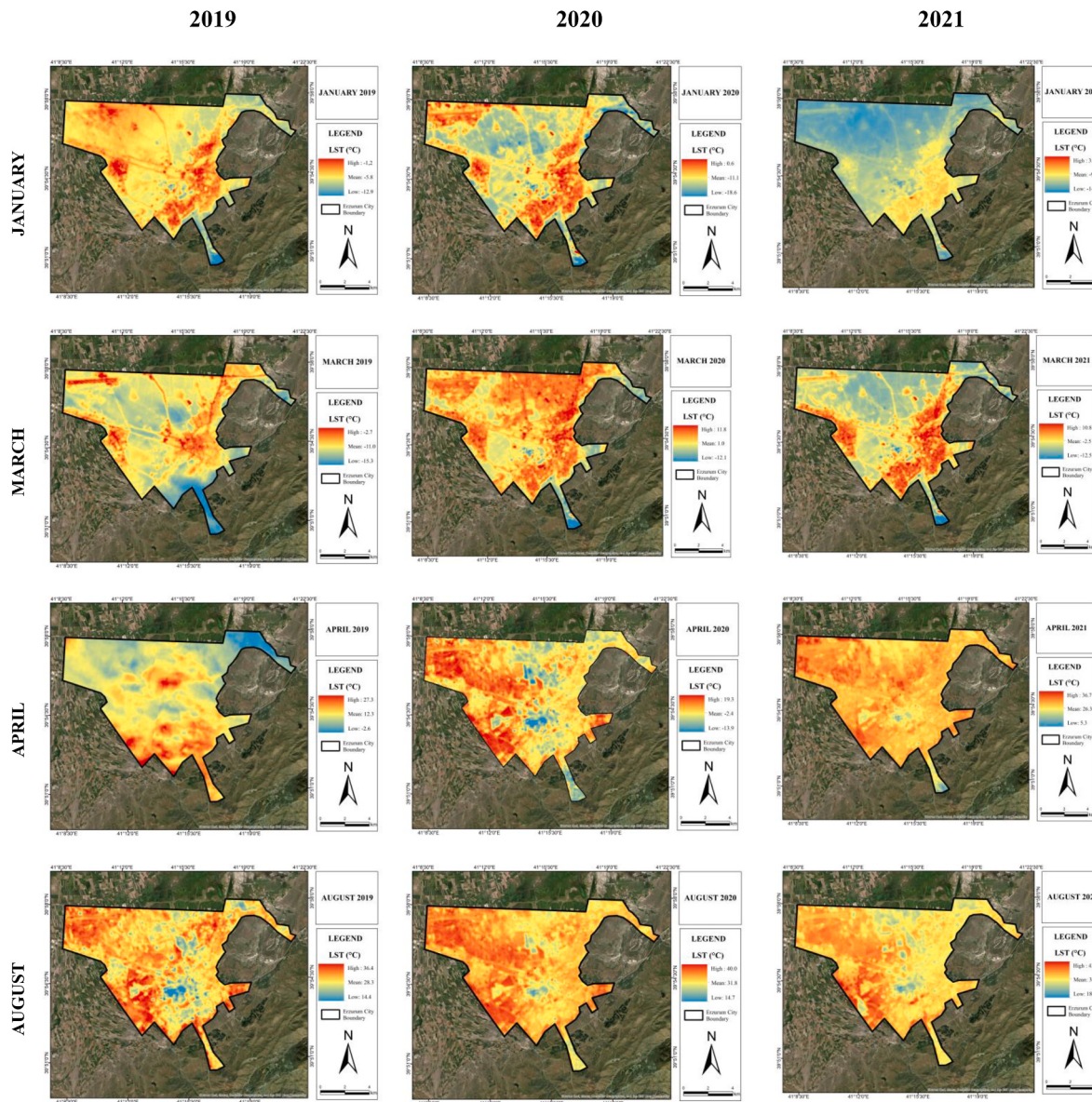


**Fig. 5.** Surface temperature distribution in Erzurum for 2019–2020–2021 January–March–April–August.

**Table 4**  
LST values of Erzurum Province for 2019, 2020 and 2021.

Land Surface Temperature (°C)													
Month	Jan			Mar			Apr			Aug			
	Year	Min	Max	Mean	Min	Max	Mean	Min	Max	Mean	Min	Max	Mean
2019		-12.9	-1.2	-5.8	-15.3	-2.7	-11	-2.6	27.3	2.3	-14.4	36.4	28.3
2020		-18.6	0.6	-11.1	-12.1	11.8	1	-13.9	39.3	-2.4	-14.7	40	31.8
2021		-14.7	3.4	9.6	-12.5	10.8	2.5	-5.3	36.7	26.3	-18.3	43.1	33.3

• High Low

was 46.17, 39.56, and 35.0  $\mu\text{g}/\text{m}^3$ , respectively. The highest average distribution of  $\text{NO}_2$  was observed in the pre-COVID-19 period in 2019, followed by a decrease in the COVID-19 period in 2020, and then a further decrease in the post-COVID-19 period in 2021. The average distribution of  $\text{O}_3$  for the years 2019, 2020, and 2021 was 24.7, 28.87, and 31.51  $\mu\text{g}/\text{m}^3$ , respectively. The lowest average distribution of  $\text{O}_3$  was observed in 2019, while the highest average distribution of  $\text{O}_3$  was detected in 2021. A continuous increase in  $\text{O}_3$  values was observed from

2019 to 2021.

The average distribution of  $\text{PM}_{10}$  for the years 2019, 2020, and 2021 was 51.42, 27.22, and 44.7  $\mu\text{g}/\text{m}^3$ , respectively. The lowest average  $\text{PM}_{10}$  distribution was observed in 2020, while the highest average  $\text{PM}_{10}$  distribution was detected in 2019. The  $\text{PM}_{10}$  value with the highest distribution average in 2019 decreased in 2020 but started to rise again in 2021. The average distribution of  $\text{SO}_2$  for the years 2019, 2020, and 2021 was 8.5, 6.08, and 7.7  $\mu\text{g}/\text{m}^3$ , respectively. The lowest average

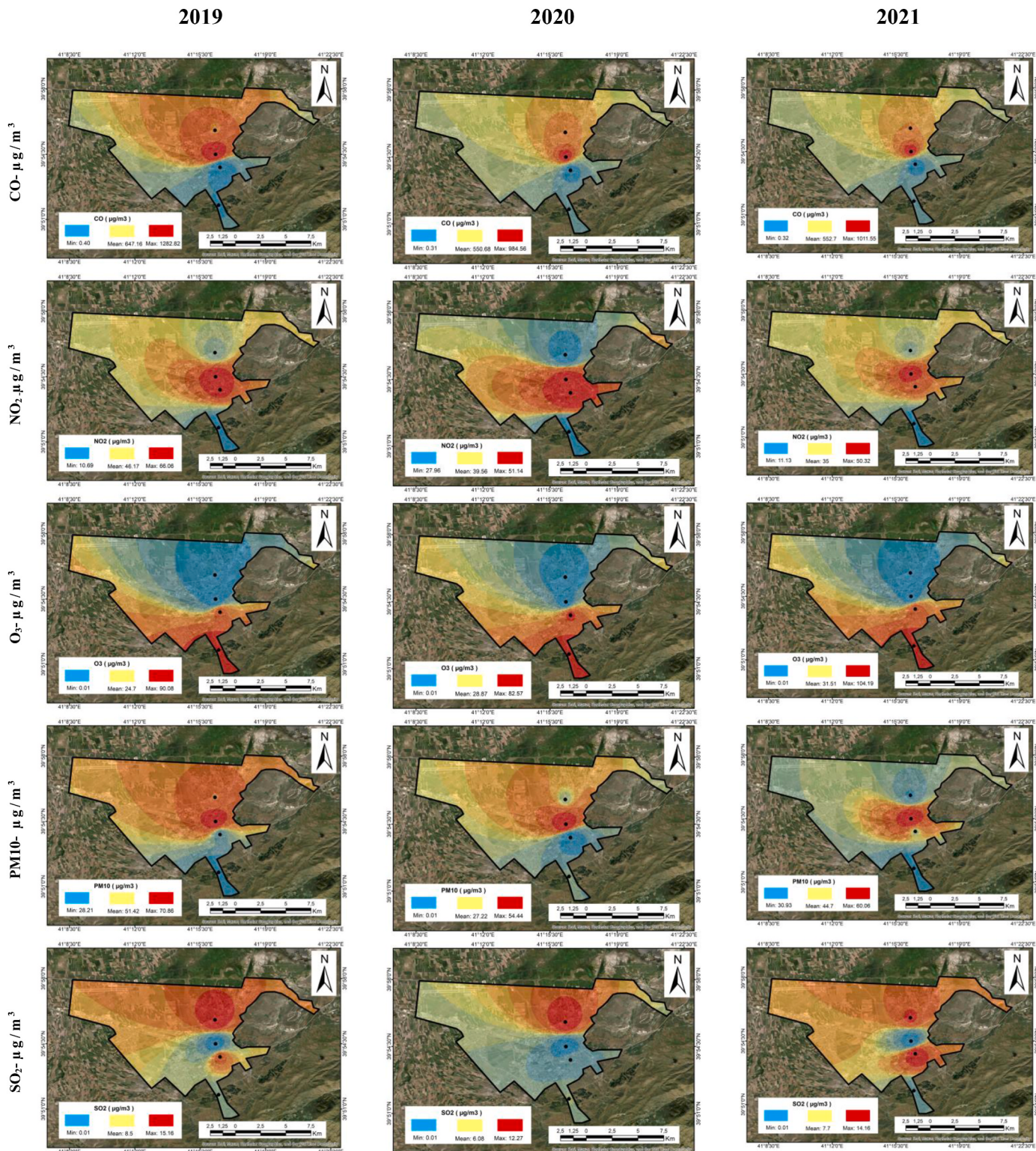


**Fig. 6.** Air pollution distribution image obtained from the ground stations in the city center.

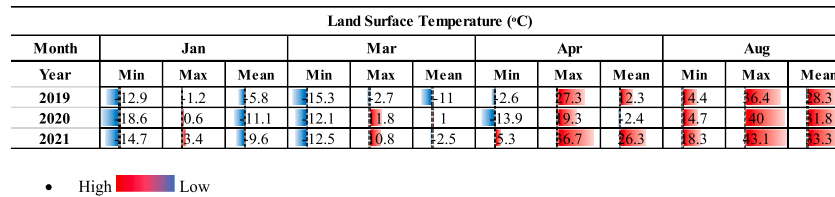
distribution of SO<sub>2</sub> was observed in 2020, while the highest average distribution of SO<sub>2</sub> was detected in 2019. The SO<sub>2</sub> value with the highest distribution average in 2019 decreased in 2020 but started to rise again in 2021.

### 3.3. Ground air temperature analysis

In the air temperature analysis, using the hourly air temperature data of January, March, April, and August of 2019, 2020, and 2021 from 16 meteorological stations in the city of Erzurum, maximum, minimum, and average air temperature maps of these months were obtained with the ArcGIS 10.4.1 program. The air temperature distribution was

**Table 5**  
Air pollution distribution obtained from the stations in the city center.

Year		CO $\mu\text{g}/\text{m}^3$	NO <sub>2</sub> $\mu\text{g}/\text{m}^3$	O <sub>3</sub> $\mu\text{g}/\text{m}^3$	PM <sub>10</sub> $\mu\text{g}/\text{m}^3$	SO <sub>2</sub> $\mu\text{g}/\text{m}^3$
2019	Min	0.4	10.69	0.01	28.21	0.01
	Max	1282.82	66.06	90.08	70.86	15.16
	Mean	647.16	46.17	24.7	51.42	8.5
2020	Min	0.31	27.96	0.01	0.01	0.01
	Max	984.56	51.14	82.57	54.44	12.27
	Mean	550.68	39.56	28.87	27.22	6.08
2021	Min	0.32	11.13	0.01	30.93	0.01
	Max	1011.55	50.32	104.19	60.06	14.16
	Mean	552.7	35	31.51	44.7	7.7



• High      Low

**Fig. 7.** Air temperature distribution in Erzurum for 2019–2020–2021 January–March–April–August.

**Table 6**  
Air temperature of Erzurum Province for 2019, 2020, and 2021.

Mon	Meteorological Station Air Temperature ( $^{\circ}\text{C}$ )											
	Jan			Mar			Apr			Aug		
Year	Min	Max	Mean	Min	Max	Mean	Min	Max	Mean	Min	Max	Mean
2019	-7.6	-0.1	-2.9	-4.6	2.7	-0.7	-0.9	7.9	2.8	0.1	20.7	3.6
2020	-8.6	-0.1	-2.6	-0.9	3.2	0.6	0.1	5.7	1.2	0.1	20.2	7.5
2021	-7.3	-2.9	-4.9	-5.2	-0.1	-1.1	-3.8	13.4	9.8	25.7	22.4	20.2

• High      Low

depicted in maps Fig. 7 and data in Table 6. Comparing the highest temperature area in the temperature maps with ground station data showed that the topographical characteristics of the area's wind speed directly influence the occurrence of the urban heat island (UHI) effect.

Table 6 displays the average air temperature values for January in the years 2019, 2020, and 2021, which were  $-2.9^{\circ}\text{C}$ ,  $-2.6^{\circ}\text{C}$ , and  $-4.9^{\circ}\text{C}$ , respectively. In January, the highest average air temperature was recorded in 2020, whereas the lowest average air temperature was recorded in 2021. After the lockdown period, there was a  $2.3^{\circ}\text{C}$  decrease

in January's average air temperatures in 2021 compared to 2020. The average air temperature values for the month of March 2019, 2020, and 2021, were  $-0.7^{\circ}\text{C}$ ,  $0.6^{\circ}\text{C}$ , and  $-1.1^{\circ}\text{C}$ , respectively. The highest average air temperature for March was recorded in 2020, while the lowest average air temperature was observed in 2021. As per the data, a decrease of  $1.7^{\circ}\text{C}$  was identified in March average air temperatures after the lockdown period (2021) compared to the lockdown period (2020). The average air temperature for April was recorded over three years, 2019, 2020, and 2021, and was found to be  $2.8^{\circ}\text{C}$ ,  $1.2^{\circ}\text{C}$ , and  $9.8^{\circ}\text{C}$ ,

**Table 7**  
The difference in pollution parameters before, during, and after COVID-19 in 2019, 2020, and 2021.

Air Pollutants		CO	NO <sub>2</sub>	O <sub>3</sub>	PM <sub>10</sub>	SO <sub>2</sub>
Mean value 2019	Pre-COVID-19	647.16	46.17	24.7	51.42	8.5
Mean value 2020	COVID-19	550.68	39.56	28.87	27.22	6.08
Mean value 2021	Post-COVID-19	552.7	35	31.51	44.7	7.7
Values Differences						
Difference 2020-2019		-96.48	-6.61	4.17	-34.2	-242
Difference 2021-2020		2.02	-4.56	2.64	-12.48	1.62
Difference 2021-2019		-94.46	-11.17	6.81	-6.72	-0.8
Differences in (%)						
Difference of COVID-19 period before COVID-19 (%)		-14.9	-14.3	16.9	-7.1	-28.5
Difference of Post-COVID and COVID period (%)		0.4	-11.5	9.1	-64.2	26.6
Difference between Post-COVID-19 and Pre-COVID-19 (%)		-14.6	-24.2	27.6	-3.1	-9.4

• High      Low

respectively. The highest average air temperature for April was observed in 2021, whereas the lowest average air temperature was observed in 2020. Notably, the average air temperature in April 2021 showed an increase of 8.6 °C when compared to the previous year. However, the air temperature declined by 1.6 °C during the lockdown in 2020 compared to 2019.

The mean air temperatures for August 2019, 2020, and 2021 were 3.6 °C, 7.5 °C, and 20.2 °C, respectively. The maximum average air temperature for August was recorded in 2021, whereas the minimum was recorded in 2019. The average air temperature values for the month of August have steadily increased from 2019 to 2021. Compared to August 2020, there was a rise of 12.7 °C in the average air temperature in August 2021 (Table 6).

Air pollution parameters during the pre-COVID, COVID, and post-COVID periods are shown in Table 7. The CO level, which was 647.16 µg/m<sup>3</sup> during the pre-COVID period, decreased by 14.9%–550.68 µg/m<sup>3</sup> during the lockdown period. Our findings are consistent with those of previous studies that reported CO reductions ranging from -7% to -84% during lockdowns (-11% (Liu et al., 2021), -25% (Dutheil et al., 2020), -26.5% (Garcia et al., 2022), -27.25% (Allu et al., 2021), -64.8% (Nakada and Urban, 2020) and -84% (Mete et al., 2022)). Notably, while the CO level decreased by 64.8% in humid subtropical São Paulo, Brazil, it decreased by 84% in hot and temperate Adana, Turkey. Our findings suggest that the reductions in CO levels were greater in cities with warm climates compared to those with colder climates during the lockdown period.

Following the COVID-19 period, there was a slight increase of 0.4% in CO values compared to the lockdown period. However, the CO value after the COVID-19 period still showed a significant decrease of 14.6% compared to the pre-lockdown period.

During the pre-COVID-19 period, the NO<sub>2</sub> value was measured at 46.17 µg/m<sup>3</sup>, and it decreased by 14.3%–39.56 µg/m<sup>3</sup> during the lockdown period. This finding is consistent with the results of several other studies, including Bray et al. (2021) (-9.19%), Liu et al. (2021) (-23.37%), Dutheil et al. (2020) (-30%), Allu et al. (2021) (-33.7%), Garcia et al. (2022) (-44%), and Nakada and Urban (2020) (-54.3%). After the COVID-19 period, the NO<sub>2</sub> value decreased by 24.2% compared to the pre-lockdown period.

During the lockdown period, the PM<sub>10</sub> value decreased by 47.1% from its pre-COVID-19 value of 51.42 µg/m<sup>3</sup> to 27.22 µg/m<sup>3</sup>. This finding is consistent with other studies that reported PM<sub>10</sub> reductions of

0.35% (Mete et al., 2022), 14–20% (Liu et al., 2021), and 38.3% (Garcia et al., 2022). However, after the lockdown period, the PM<sub>10</sub> value increased to 44.7 µg/m<sup>3</sup>.

During the pre-COVID-19 period, the SO<sub>2</sub> value was 8.5 µg/m<sup>3</sup>, and it decreased by 28.5% to 6.08 µg/m<sup>3</sup> during the lockdown period. This finding is consistent with other studies that found a decrease in SO<sub>2</sub> values ranging from 2 to 20% (Liu et al., 2021), 23.6% (Mete et al., 2022), and 33.5% (Garcia et al., 2022). However, after the lockdown period, the SO<sub>2</sub> value increased to 7.7 µg/m<sup>3</sup>. During the lockdown period, the O<sub>3</sub> environmental variable, which was 24.7 µg/m<sup>3</sup> in the pre-COVID-19 period, showed an increase of 16.9% to reach 28.87 µg/m<sup>3</sup>. After the lockdown period, it continued to increase to 31.51 µg/m<sup>3</sup>. Other studies have reported an increase in O<sub>3</sub> ratio ranging from 5.9% (Garcia et al., 2022) to 10–27% (Liu et al., 2021) and 30% (Nakada and Urban, 2020), which is consistent with the results of our study. However, Mete et al. (2022) reported a decrease of 68.4% in their study.

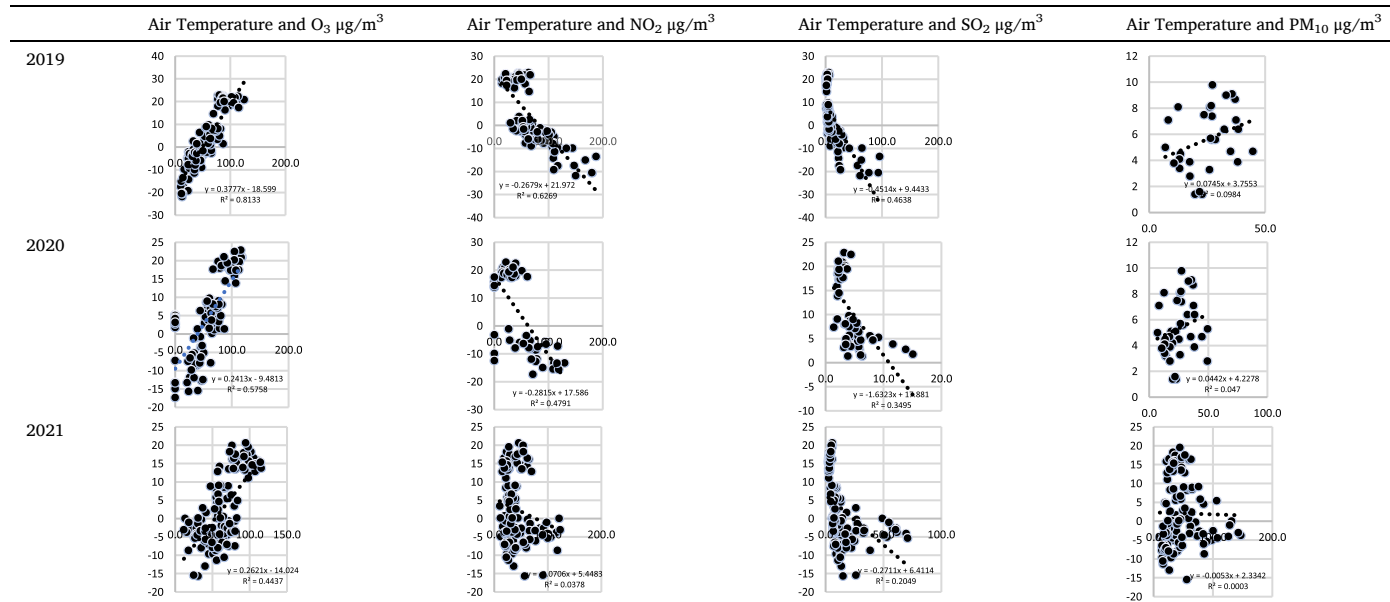
In Erzurum city, the first COVID-19 case was reported in late March of 2020, leading to the implementation of various measures across the country, including Erzurum. The average land surface temperature (LST) in April 2020 was -2.4 °C, significantly lower than the average LST value of 12.3 °C recorded in April 2019. The strict restrictions in place during April led to this significant decrease in the average LST value. It is worth noting that the LST value in Erzurum during April was higher than the values (-4.6 °C and -1 °C) recorded in Andalusia, Spain (Garcia et al., 2022) and Montreal, Canada (Teufel et al., 2021), respectively.

### 3.3.1. Statistical analyses

The correlations between air pollution and air temperature during the pre-COVID-19, COVID-19, and post-COVID-19 periods were statistically defined. The correlation of the air temperature with the O<sub>3</sub>, NO<sub>2</sub>, SO<sub>2</sub>, and PM<sub>10</sub> pollutants for January, March, April, and August of 2019, 2020, and 2021 was evaluated using the coefficient of determination ( $R^2$ ). As shown in Table 8, there is a positive correlation between the air temperature and O<sub>3</sub>. The air temperature level increases when the O<sub>3</sub> rate increases. The air temperature and O<sub>3</sub> are higher in level and have a strong positive correlation in 2019 before the COVID-19 outbreak, a correlation of  $R^2 = 0.8$ , and during the COVID-19 breakdown in 2020, the correlation is 0.6 and in post-COVID-19, the  $R^2 = 0.44$ . Consequently, the air temperature in 2019 increased as a result of high emissions of O<sub>3</sub>, whereas the air temperature was lower during 2020 and during 2021 and had a medium positive correlation with O<sub>3</sub> due to low

Table 8

Correlation analysis between the air temperature and air pollution variables of O<sub>3</sub> µg/m<sup>3</sup>, NO<sub>2</sub> µg/m<sup>3</sup>, SO<sub>2</sub> µg/m<sup>3</sup> and PM<sub>10</sub> µg/m<sup>3</sup>.



emissions caused by the lockdown and its significant effect on lowering pollution levels. This result confirms the published findings that indicate that  $O_3$  emissions impact the air temperature degree and physiological equivalent temperature PET level (Yilmaz et al., 2022). Nevertheless, a stronger medium negative correlation exists between air temperature and  $NO_2$  and  $SO_2$  emissions,  $R^2 = 0.6$  and 0.5, respectively. The air temperature level decreases when they increase. For  $NO_2$ ,  $SO_2$ , and air temperature, there was a low correlation during COVID-19 in 2020,  $R^2 = 0.5$  and 0.35, respectively, and during 2021,  $R^2 = 0.37$  and  $R_2 = 0.2$ , respectively. There is no correlation between air temperature and  $PM_{10}$  because the scatter points are fragmented.

#### 4. Conclusion

The COVID-19 outbreak and ensuing global lockdown situation have generated a very negative impact on the world economy, but they have also lent us a unique opportunity to research and better grasp the impacts of human activity on environmental pollution and urban climates. This study investigates the air pollution and the thermal environment effects on the cold region of Erzurum City, Turkey, during COVID-19 2020 and before 2019, and after 2021.

Other studies have generally examined the relationship between the COVID-19 pandemic and air pollutants, but there is a lack of research on the relationship between air pollutants, air temperatures, and ground temperatures. This study is unique in analyzing these relationships. Additionally, while other studies have focused on the comparison between the COVID-19 period and the lockdown period, or the lockdown period and the post-COVID-19 period, our study examines the pre-COVID-19 period, lockdown period, and post-lockdown period over a three-year span, setting it apart from previous research.

It has been observed that the topographic structure is more effective in forming air pollution in Erzurum, a cold climate region. The effect of curfews or restrictions made during the pandemic period was not reflected in the air pollution values measured in the city. People have been observed to stay in their homes, which causes more fuel consumption for heating purposes in winter. The fact that the prevailing wind speed is 2.7 m/s on average and that this value is even lower in winter months cannot prevent the distribution of pollution.

In this study, conducted in Erzurum Province, air pollution, land surface temperature, air temperature, and statistical analyses were performed to reveal the effects of the measures and restrictions against the COVID-19 epidemic that emerged at the end of 2019 on the cities in cold regions.

As a result of these analyses, some results have emerged. Compared to the pre-COVID-19 era,  $CO$ ,  $NO_2$ ,  $PM_{10}$ , and  $SO_2$  values decreased by 14.9%, 14.3%, 47.1%, and 28.5%, respectively, while the  $O_3$  value increased by 16.9% during the lockdown period. A positive correlation was determined between air temperature and  $O_3$ . While it had a strong positive correlation before the COVID-19 outbreak in 2019, there was a weaker correlation post-COVID-19. In short, while the air temperature increased in 2019 as a result of higher  $O_3$  emissions, the air temperature was lower in 2020 and beyond. It has a moderately positive correlation with the effect of low  $O_3$  emissions caused by quarantine. However, a stronger moderate negative correlation was obtained between air temperature and  $NO_2$  and  $SO_2$  emissions, with  $R^2 = 0.6$  and 0.5, respectively. There is no correlation between air temperature and  $PM_{10}$  because the scatter points are fragmented. The average LST value decreased significantly in April when the restrictions were intense; the average LST value (-2.4 °C) in April 2020 was lower than that in 2019 which recorded 12.3 °C, with LST differences of roughly 14.7 °C.

This study concludes that the integration of remote sensing data and GIS is a useful tool in urban LST detection in cold climate zones. By adhering to sustainable transport plans and clean air policies, the urban environment could be improved due to declining atmospheric pollutants and less urban heat stress. Therefore, polluted air stays above the city, especially in winter, reducing the air quality of the environment. The

thermal infrared bands of Landsat 8 data and official products present higher average LSTs than those obtained through meteorological stations. They show high precision and low sensitivity, working well on a global scale. They may therefore be considered adequate for estimating the LST of the city in the cold region. Nevertheless, it is necessary to carry out further applied research to validate the precision of these products in cities located in another cold region.

#### Declaration of Competing interest

The authors declare that they have no known competing financial interests or personal relationships that could have appeared to influence the work reported in this paper.

#### Data availability

No data was used for the research described in the article.

#### Acknowledgments

The authors present their special thanks to "The Scientific and Technological Research Council of Turkey, TÜBİTAK under Project No: 2150627 and Project No: 119O479" and the Turkish State Meteorological Service (MGM) for sharing their data free of charge. The authors present their special thanks to the Turkish State Meteorological Service (DMI) for sharing their data free of charge. We would like to also thank the Environment and Urban Ministry, General Directorate of Environmental Management, Laboratory, Measurement and Monitoring Department, Clean Air Center (CAC) "Air Quality Preliminary Studies" for helping us with the pollution data of the city of Erzurum, which we needed in the early stages of the project, and for sharing their valuable measurement results with us.

#### References

- Allu, S.K., Reddy, A., Srinivasan, S., Maddala, R.K., Anupoju, G.R., 2021. Surface ozone and its precursor gases concentrations during COVID-19 lockdown and pre-lockdown periods in hyderabad city, India. *Environmental Processes* 8 (2), 959–972.
- Amanollahi, J., Tzanis, C., Ramlı, M.F., Abdullah, A.M., 2016. Urban heat evolution in a tropical area utilizing Landsat imagery. *Atmos. Res.* 167, 175–182.
- Analitis, A., De' Donato, F., Scortichini, M., Lanki, T., Basagana, X., Ballester, F., et al., 2018. Synergistic effects of ambient temperature and air pollution on health in Europe: results from the PHASE project. *Int. J. Environ. Res. Publ. Health* 15 (9), 1856.
- Anonymous, 2023. [http://www.nik.com.tr/content\\_sistem\\_uydu.asp?id=49](http://www.nik.com.tr/content_sistem_uydu.asp?id=49).
- Arslan, G., Yıldırım, M., Tanhan, A., Bulut, M., Allen, K.A., 2021. Coronavirus stress, optimism-pessimism, psychological inflexibility, and psychological health: psychometric properties of the Coronavirus Stress Measure. *Int. J. Ment. Health Addiction* 19 (6), 2423–2439.
- Avdan, U., Jovanovska, G., 2016. Algorithm for automated mapping of land surface temperature using LANDSAT 8 satellite data. *Journal of Sensors* 1–8, 1480307.
- Bao, R., Zhang, A., 2020. Does lockdown reduce air pollution? Evidence from 44 cities in northern China. *Sci. Total Environ.* 731, 139052.
- Bandyopadhyay, S., 2020. Coronavirus Disease 2019 (COVID-19): we shall overcome. *Clean Technol. Environ. Policy* 22 (3), 545–546.
- Beloconi, A., Vounatsou, P., 2023. Long-term air pollution exposure and COVID-19 case-severity: an analysis of individual-level data from Switzerland. *Environ. Res.* 216, 114481.
- Bharath, H.A., Chandan, M.C., Nimish, G., 2019. Assessing land surface temperature and land use change through spatio-temporal analysis: a case study of select major cities of India. *Arabian J. Geosci.* 12 (11), 367.
- Bray, C.D., Nahas, A., Battye, W.H., Aneja, V.P., 2021. Impact of lockdown during the COVID-19 outbreak on multi-scale air quality. *Atmos. Environ.* 254, 118386.
- Chandan, M.C., Nimish, G., Bharath, H.A., 2019. Analysing spatial patterns and trend of future urban expansion using SLEUTH. *Spatial Inf. Res.* 7, 1–13. <https://doi.org/10.1007/s41324-019-00262-4>.
- Chen, F., Yang, X., Zhu, W., 2014a. WRF simulations of urban heat island under hot-weather synoptic conditions: the case study of Hangzhou City, China. *Atmos. Res.* 138, 364–377.
- Chen, A., Yao, X.A., Sun, R., Chen, L., 2014b. Effect of urban green patterns on surface urban cool islands and its seasonal variations. *Urban For. Urban Green.* 13 (4), 646–654. <https://doi.org/10.1016/j.ufug.2014.07.006>.
- Cui, Y., Zhang, Z.F., Froines, J., Zhao, J., Wang, H., Yu, S.Z., Detels, R., 2003. Air pollution and case fatality of SARS in the People's Republic of China: an ecologic study. *Environ. Health* 2 (1), 1–5.

- De, B., Mukherjee, M., 2018. Optimisation of canyon orientation and aspect ratio in warm-humid climate: case of Rajarhat Newtown, India. *Urban Clim.* 24, 887–920.
- Dutheil, F., Baker, J.S., Navel, V., 2020. COVID-19 as a factor influencing air pollution? *Environ. Pollut.* 263, 114466.
- Du, H., Cai, W., Xu, Y., Wang, Z., Wang, Y., Cai, Y., 2017. Quantifying the cool island effects of urban green spaces using remote sensing Data. *Urban For. Urban Green.* 27, 24–31. <https://doi.org/10.1016/j.ufug.2017.06.008>.
- Ekanayake, A., Rajapaksha, A.U., Hewawasam, C., Anand, U., Bontempi, E., Kurwadkar, S., Vithanage, M., 2023. Environmental Challenges of COVID-19 Pandemic: Resilience and Sustainability—A Review. *Environmental research,* 114496.
- Fofana, N.K., Latif, F., Sarfraz, S., Bashir, M.F., Komal, B., 2020. Fear and agony of the pandemic leading to stress and mental illness: an emerging crisis in the novel coronavirus (COVID-19) outbreak. *Psychiatr. Res.* 291, 113230.
- Garcia, E., Marian, B., Chen, Z., Li, K., Lurmann, F., Gilliland, F., Eckel, S.P., 2022. Long-term air pollution and COVID-19 mortality rates in California: findings from the Spring/Summer and Winter surges of COVID-19. *Environ. Pollut.* 292, 118396.
- García, D.H., Díaz, J.A., 2022. Impacts of the COVID-19 confinement on air quality, the Land Surface Temperature and the urban heat island in eight cities of Andalusia (Spain). *Remote Sens. Appl.: Society and Environment* 25, 100667.
- Guha, S., Govil, H., Besoya, M., 2020. An investigation on seasonal variability between LST and NDWI in an urban environment using Landsat satellite data. *Geomatics, Nat. Hazards Risk* 11 (1), 1319–1345.
- Harmay, N.S.M., Kim, D., Choi, M., 2021. Urban heat island associated with land use/land cover and climate variations in Melbourne, Australia. *Sustain. Cities Soc.* 69, 102861.
- Huang, Y., Lei, C., Liu, C.H., Perez, P., Forehead, H., Kong, S., Zhou, J.L., 2021. A review of strategies for mitigating roadside air pollution in urban street canyons. *Environ. Pollut.* 280, 116971.
- Irmak, M.A., Yilmaz, S., Mutlu, E., Yilmaz, H., 2020. Analysis of different urban spaces on thermal comfort in cold regions: a case from Erzurum. *Theor. Appl. Climatol.* 141 (3), 1593–1609.
- Ilyas, S.Z., Khattak, A.I., Nasir, S.M., Qurashi, T., Durrani, R., 2010. Air pollution assessment in urban areas and its impact on human health in the city of Quetta, Pakistan. *Clean Technol. Environ. Policy* 12 (3), 291–299.
- Javanroodi, K., Nik, V.M., 2020. Interactions between extreme climate and urban morphology: investigating the evolution of extreme wind speeds from mesoscale to microscale. *Urban Clim.* 31, 100544.
- Jongtanom, Y., Kositanon, C., Baulert, S., 2011. Temporal variations of urban heat island intensity in three major cities, Thailand. *Mod. Appl. Sci.* 5, 105–110.
- Koç, A., Yilmaz, S., 2020. Landscape character analysis and assessment at the lower basin-scale. *Appl. Geogr.* 125, 102359.
- Li, C., Wang, Z., Li, B., Peng, Z.R., Fu, Q., 2019. Investigating the relationship between air pollution variation and urban form. *Build. Environ.* 147, 559–568.
- Li, J.J., Wang, X.R., Wang, X.J., Ma, W.C., Zhang, H., 2009. Remote sensing evaluation of urban heat island and its spatial pattern of the Shanghai metropolitan area, China. *Ecol. Complex.* 6 (4), 413–420.
- Li, G., Zhang, H., Hu, M., He, J., Yang, W., Zhao, H., et al., 2022. Associations of combined exposures to ambient temperature, air pollution, and green space with hypertension in rural areas of Anhui Province, China: a cross-sectional study. *Environ. Res.* 204, 112370.
- Liu, F., Wang, M., Zheng, M., 2021. Effects of COVID-19 lockdown on global air quality and health. *Sci. Total Environ.* 755, 142533.
- Mete, B., Acar, O., Kanat, C., Doğan, E., 2022. The effect of measures taken during the COVID-19 pandemic on air pollution: a East Mediterranean example from Turkey. *Turkish Journal of Public Health* 20 (1), 129–137.
- MGM, 2019. Turkish State Meteorological Service (MGM) shared their data, 2021. <http://www.mgm.gov.tr/>.
- Ministry of Education 2021. <https://www.meb.gov.tr/en/>. <https://www.meb.gov.tr/covid-19-vaccination-of-teachers-and-school-workers-continues/haber/23201/en>.
- Ministry of Education, 2020. Mart 2020; dünya sağlık örgütü. Coronavirus disease 2019 (COVID-19) situation report – 54. Rapor numarası: 54. <https://www.tccb.gov.tr/>, 2020. [internet]. İsviçre: Dünya Sağlık Örgütü; 2020.
- MoEU, 2017. [http://www.cevresehirkutuphanesi.com/assets/files/slider\\_pdf/ro1\\_7bNm6tR8](http://www.cevresehirkutuphanesi.com/assets/files/slider_pdf/ro1_7bNm6tR8). ÖzTÜRK, M.
- MoEU, 2022. Republic of Turkey, Ministry of Environment and Urbanisation (CSB). <http://mobil.air.gov.tr/Default.ltr.aspx>. [http://www.who.int/topics/air\\_pollution/en](http://www.who.int/topics/air_pollution/en).
- Mor, S., Kumar, S., Singh, T., Dogra, S., Pandey, V., Ravindra, K., 2021. Impact of COVID-19 lockdown on air quality in Chandigarh, India: understanding the emission sources during controlled anthropogenic activities. *Chemosphere* 263, 127978.
- Nakada, L.Y.K., Urban, R.C., 2020. COVID-19 pandemic: impacts on the air quality during the partial lockdown in São Paulo state, Brazil. *Sci. Total Environ.* 730, 139087.
- Nikolopoulou, M., Lykoudis, S., 2006. Thermal comfort in outdoor urban spaces: analysis across different European countries. *Build. Environ.* 41 (11), 1455–1470.
- Nikolopoulou, M., Steemers, K., 2003. Special issue on urban research, Thermal comfort and psychological adaptation as a guide for designing urban spaces. *Energy Build.* 35 (1), 95–101.
- Okumus, D.E., Terzi, F., 2021. Evaluating the role of urban fabric on surface urban heat island: the case of Istanbul. *Sustain. Cities Soc.* 73, 103128.
- Parida, B.R., Bar, S., Kaskaoutis, D., Pandey, A.C., Polade, S.D., Goswami, S., 2021. Impact of COVID-19 induced lockdown on land surface temperature, aerosol, and urban heat in Europe and North America. *Sustain. Cities Soc.* 75, 103336.
- Qaid, A., Bashir, M.F., Remaz Ossen, D., Shahzad, K., 2022. Long-term statistical assessment of meteorological indicators and COVID-19 outbreak in hot and arid climate, Bahrain. *Environmental Science and Pollution Research* 29 (1), 1106–1116.
- Ravindra, K., Singh, T., Vardhan, S., Shrivastava, A., Singh, S., Kumar, P., Mor, S., 2022. COVID-19 pandemic: what can we learn for better air quality and human health? *Journal of infection and public health* 15 (2), 187–198.
- Reis, C., Lopes, A., Nouri, A.S., 2022. Assessing urban heat island effects through local weather types in Lisbon's Metropolitan Area using big data from the Copernicus service. *Urban Clim.* 43, 101168.
- Rendana, M., Idris, W.M.R., Rahim, S.A., 2021. Spatial distribution of COVID-19 cases, epidemic spread rate, spatial pattern, and its correlation with meteorological factors during the first to the second waves. *Journal of Infection and Public Health* 14 (10), 1340–1348.
- Sari, E., Yilmaz, S., 2021. The effect on air pollution distribution of wind in different street canyons: the case of Erzurum. *Planlama-Planning* 31 (3).
- Shanshan, C.H.E.N., Haase, D., Qureshi, S., Firozjael, M.K., 2022. Integrated Land Use and Urban Function Impacts on Land Surface Temperature: Implications on Urban Heat Mitigation in Berlin with Eight-type Spaces. *Sustainable Cities and Society*, 103944.
- Shehzad, K., Xiaoxing, L., Ahmad, M., Majeed, A., Tariq, F., Wahab, S., 2021. Does air pollution upsurge in megacities after COVID-19 lockdown? A spatial approach. *Environ. Res.* 197, 111052.
- Shi, Y., Xie, X., Fung, J.C.H., Ng, E., 2018. Identifying critical building morphological design factors of street-level air pollution dispersion in high-density built environment using mobile monitoring. *Build. Environ.* 128, 248–259.
- Sicard, P., De Marco, A., Agathokleous, E., Feng, Z., Xu, X., Paoletti, E., et al., 2020. Amplified ozone pollution in cities during the COVID-19 lockdown. *Sci. Total Environ.* 735, 139542.
- Teufel, B., Sushama, L., Poitras, V., Dukhan, T., Béclair, S., Miranda-Moreno, L., Bitsuamlak, G., 2021. Impact of COVID-19-related traffic slowdown on urban heat characteristics. *Atmosphere* 12 (2), 243.
- Unger, J., 1999. Comparisons of urban and rural bioclimatological conditions in the case of a Central-European city. *Int. J. Biometeorol.* 43 (3), 139–144.
- UN., 2019. World Urbanization Prospects 2018: Highlights (ST/ESA/SER. A/421). Nations, U. (2019. (Accessed 16 October 2019).
- Venter, Z.S., Aunan, K., Chowdhury, S., Lelieveld, J., 2020. COVID-19 lockdowns cause global air pollution declines. *Proc. Natl. Acad. Sci. USA* 117 (32), 18984–18990.
- Wang, P., Chen, K., Zhu, S., Wang, P., Zhang, H., 2020. Severe air pollution events not avoided by reduced anthropogenic activities during COVID-19 outbreak. *Resour. Conserv. Recycl.* 158, 104814.
- Wang, G., Cheng, S., Wei, W., Yang, X., Wang, X., Jia, J., et al., 2017. Characteristics and emission-reduction measures evaluation of PM2. 5 during the two major events: APEC and Parade. *Sci. Total Environ.* 595, 81–92.
- Weng, Q., Liu, H., Lu, D., 2007. Assessing the effects of land use and land cover patterns on thermal conditions using landscape metrics in city of Indianapolis, United States. *Urban Ecosyst.* 10 (2), 203–219.
- Yang, J., Shi, B., Zheng, Y., Shi, Y., Xia, G., 2020. Urban form and air pollution disperse: key indexes and mitigation strategies. *Sustain. Cities Soc.* 57, 101955.
- Yilmaz, S., Mutlu, B.E., Aksu, A., Mutlu, E., Qaid, A., 2021a. Street design scenarios using vegetation for sustainable thermal comfort in Erzurum, Turkey. *Environ. Sci. Pollut. Control Ser.* 28 (3), 3672–3693.
- Yilmaz, S., Sezen, I., Sari, E.N., 2021b. The relationships between ecological urbanization, green areas, and air pollution in Erzurum/Turkey. *Environ. Ecol. Stat.* 28 (4), 733–759.
- Yilmaz, S., Irmak, M.A., Qaid, A., 2022. Assessing the effects of different urban landscapes and built environment patterns on thermal comfort and air pollution in Erzurum city, Turkey. *Build. Environ.* 219, 109210 <https://doi.org/10.1016/j.buildenv.2022.109210>.
- Zoran, M.A., Savastru, R.S., Savastru, D.M., Tautan, M.N., Baschir, L.A., Tenciu, D.V., 2022. Assessing the impact of air pollution and climate seasonality on COVID-19 multiwaves in Madrid, Spain. *Environ. Res.* 203, 111849.